DRAGON SIMULATION OF A RADIAL PWR REFLECTOR

N. Bejaoui and G. Marleau

Institut de génie nucléaire, École Polytechnique de Montréal C.P. 6079, succ. Centre-ville, Montréal, Québec, CANADA H3C 3A7

Abstract

In order to reduce the uncertainties in PWR core power distribution calculations carried out by a core code, an accurate model of the radial PWR reflector is required. The method we propose in this paper is to use a 2D transport calculation for a multi-assembly representation of the core to evaluate two groups cross sections and diffusion coefficients for the homogenized reflector. Those parameters are then injected in the core calculation to solve the diffusion equation. Here, we will compare the results obtained using the lattice code DRAGON for two groups reflector parameters with those published in the literature for the TMI-PWR benchmark.

1. Introduction

The evaluation of the power distribution in a reactor is generally based on 3D 2 groups flux solution to the diffusion equation over the full core. In fact, the PWR core is made up of many pin cells that contain fuel, clad and coolant, all arranged in assemblies. However, the peripheral zone of the core is more complicated containing the baffle, the core barrel, the neutron pad and water reflector. In general, for core calculations, assembly averaged cross sections and diffusion coefficients are considered, the reflector being also represented by a homogeneous region. For assembly or pin cross sections, a flux volume homogenization is considered based on the solution to the transport equation assuming that the assembly is repeated to infinity. The simple homogenization technique is not entirely reliable for the reflector or for assemblies located near the reflector since it does not take into account the strong coupling between the reflector and the fuel.

In the literature, there exist several methods [1, 2] to simulate the effect of the reflector zone in core calculations. One example is the use of group dependent albedos calculated in diffusion or transport [2]. In this study, we adopt a simulation model that describes the reflector explicitly in a multi-assembly environment coupled with a multi-region homogenization method.

In the next section, we first present and describe the lattice cell calculation model that will be used for reflector cross section homogenization. Then, we describe how this method is applied to the TMI-PWR benchmark problem [3]. In Section 4 we present our results and in Section 5 we conclude.

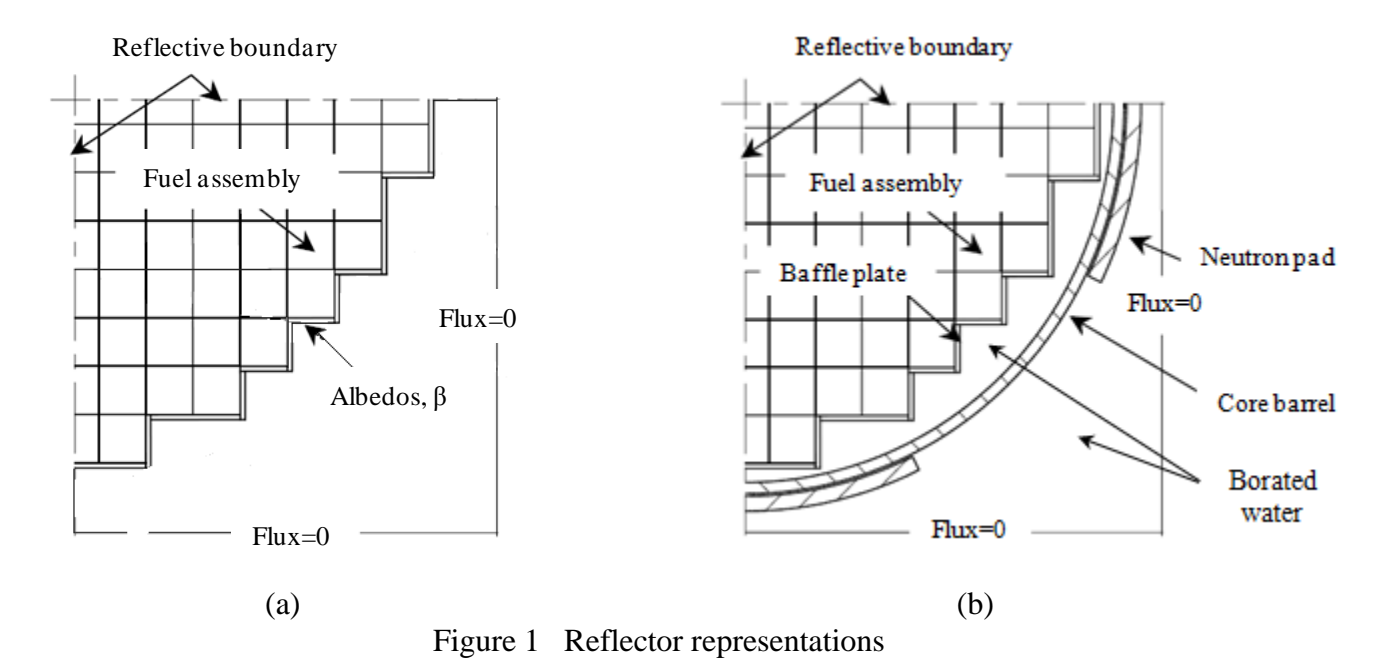
2. Methodology

Modeling exactly a PWR reactor is complex because its geometry is very heterogeneous containing fuel assemblies and the moderator. In addition, structures and fluids (baffle plate, core barrel, neutron pad and borated water) that are used to prevent neutron leakage and damage

to the vessel are also present as shown in Figure 1. The only part responsible for the production of energy in the core being the fuel, for safety analysis or refueling purpose, it is generally not necessary to determine the flux in the reflector. However, the presence of this reflector affects the flux distribution in the core thereby having an effect on the power distribution in the reactor. We can consider two different techniques to represent the effect of the reflector:

- 1- Imposing boundary conditions at the periphery of the core [2]: the reflector is represented implicitly (see Fig. 1a).
- 2- Represent the reflector by a homogeneous medium (equivalent reflector) that has the same effect on the core as the heterogeneous reflector.

Here, we choose the second technique where we consider the simplest possible geometry, that is to say homogeneous and infinite representing the true transport properties of the radial reflector. In fact, the practical utility of the parameters generated by this method may be restricted if they are sensitive to local core conditions especially the core corners. In this respect, the so-called equivalent reflector method has been quite successful (See Fig. 1b) [4]. Our model also takes into account neutron leakage.



The equivalent reflector properties were generated using a systematic procedure developed previously [4] that we adapt to the DRAGON cell code [5]. In the past, these group constants were typically treated as empirical parameter. This work follows a methodology that consists of three steps:

- 1. In the first step, we determine the homogenized cross sections of a homogeneous infinite assembly. In case of reactor at full power, this represents the assembly in the center of the core. This is used for two purposes: 1) to generate the 2-groups cross sections of the fuel assemblies in core calculation and 2) to generate the multi-group assembly cross sections for the 2-D reflector model.
- 2. In the second step, calculations are performed in transport for a 2-D geometry that

involves several fuel assemblies, the central assemblies being homogenized according to step 1 while an explicit model is used for assemblies located near the reflector and the various regions of the reflector (see Fig.2). This particular choice of homogenization depends on the type of fuel assemblies and has been found adequate for the purpose of obtaining environment-dependent reflector parameters.

3. In the third step, the real reflector is replaced in full core diffusion calculations by the properties of the equivalent reflector namely the two-group cross sections and diffusion coefficients that should reproduce the correct core leakage.

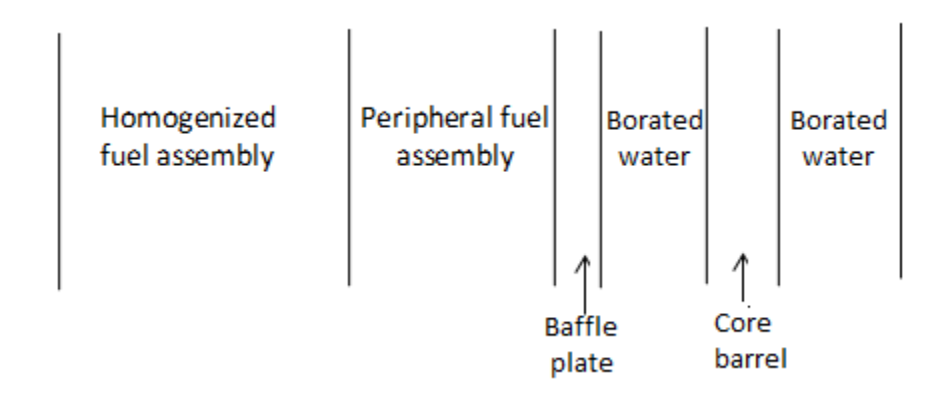


Figure 2 Reference 2-D problem with central homogenized lattice

The procedure we just described has been implemented using the lattice code DRAGON that can solve the transport equation by the method of collision probabilities (CP) [6]. The tracking module we consider is NXT: that can treat the complex geometries required in this modeling. In addition, for our simulations we use white boundary conditions where the angular flux reflected on the external surfaces is assumed isotropic. For resonance self-shielding calculations we use the generalized Stamm'ler method implemented in DRAGON through the module SHI: with the Livolant Jeanpierre normalization option LJ activated (this option proves more accurate for PWR-type lattices [7]). Because we treat fission source eigenvalue problem, calculation of the diffusion coefficient is performed using the B1 homogeneous leakage option of DRAGON programmed in the FLU: module. In this case, the critical buckling is the eigenvalue with a fixed effective multiplication factor [8].

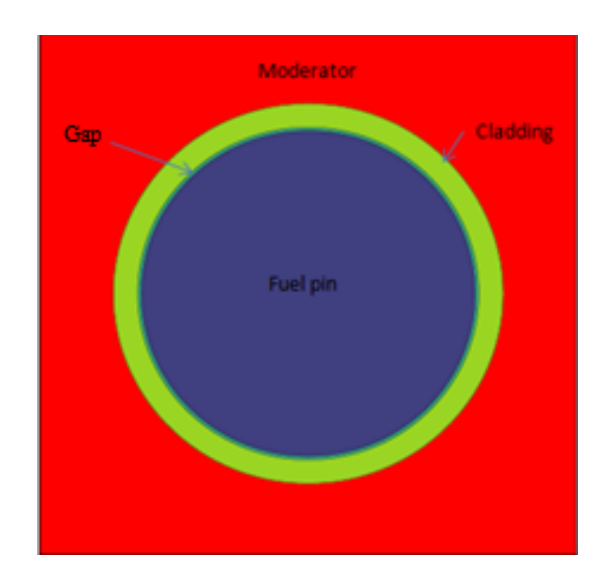
This calculation scheme is demonstrated using the pin cell benchmark case for TMI-PWR and results are compared with simulation results already published [11, 13].

3. Application to TMI-PWR benchmark

The NEA/NSC/DOC (2007)23 benchmark project is challenging and responds to the needs of estimating confidence bounds for results from simulations and analysis in real applications. The objective is to determine the uncertainty in LWR system calculations at all stages of coupled reactor physics/thermal/hydraulics calculation [3]. In this paper, we just treat the neutronic part of the exercise I. We will assume that the published Monte Carlo simulations provide the reference solutions.

3.1 TMI-PWR pin cell

Figure 3 shows the two-dimensional TMI-PWR cell benchmark problem. The geometry is a simplified unit cell representative of a typical fuel rod in a PWR reactor. This cell has a pitch of 1.4427 cm and contains the fuel (central region) followed by a gap, the cladding made of Zircaloy (0.4791 radius) and light water. White boundry conditions are applied on all external boundaries. At Hot Zero Power (HZP), the temperature is considered uniform (551°K). Table 1 list the main parameters of TMI-PWR pin-cell.

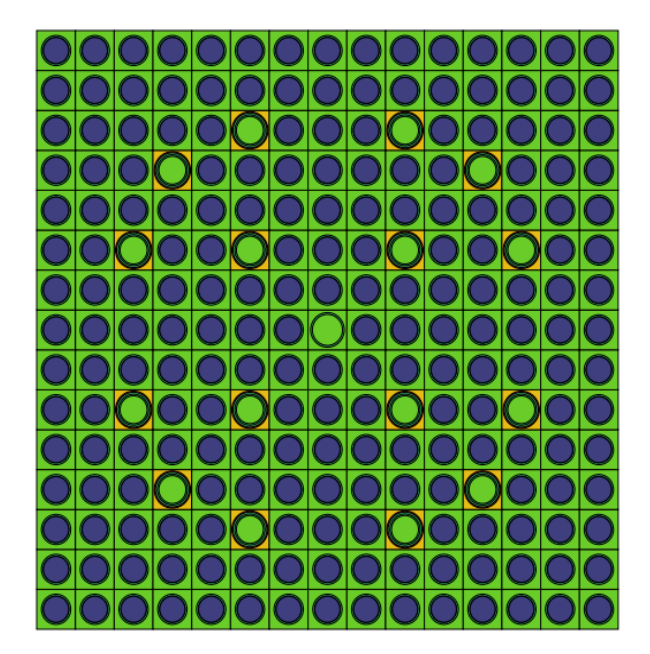


Parameter	Value
Pin-cell pitch, mm	14.427
Fuel pellet diameter, mm	9.391
Fuel pellet material	UO_2
Fuel density (95% TD), g/cm ³	10.283
Fuel enrichment, w/o	4.85
Cladding outside diameter, mm	10.928
Cladding thickness, mm	0.673
Cladding material	Zircaloy-4
Gap material	Не
Moderator material	H ₂ o

Figure 3 TMI-PWR pin cell

3.2 TMI-PWR assembly

The TMI-PWR assembly is fuelled with 3.85% enriched UO2 pellets and corresponds to the benchmark problem described in details in reference [3]. The 15x15 lattice geometry is depicted in Figure 4. It consists of 208 fuel cells, 1 instrumentation tube located in the center of the assembly and 16 guide tubes. Moreover, for the material composition, light water is used as a moderator with Zircaloy-4 as a cladding material. In the table of Figure 4, we present some important parameters required for this study.



Parameter	Value
Fuel assembly dimensions	15×15
Number of fuel rods per FA	208
Number of guide tubes per FA	16
Number of instrumentation tubes per FA	1
Fuel rod pitch, mm	14.427
Fuel rod outside diameter, mm	10.922
Fuel pellet diameter, mm	9.39
Cladding thickness, mm	0.673
Guide tube outside diameter, mm	13.462
Guide tube inside diameter, mm	12.649
Instrumentation tube outside diameter, mm	12.522
Instrumentation tube inside diameter, mm	11.201
Fuel assembly pitch, mm	218.11

Figure 4 TMI-PWR fuel assembly

3.3 TMI-PWR reflected assembly

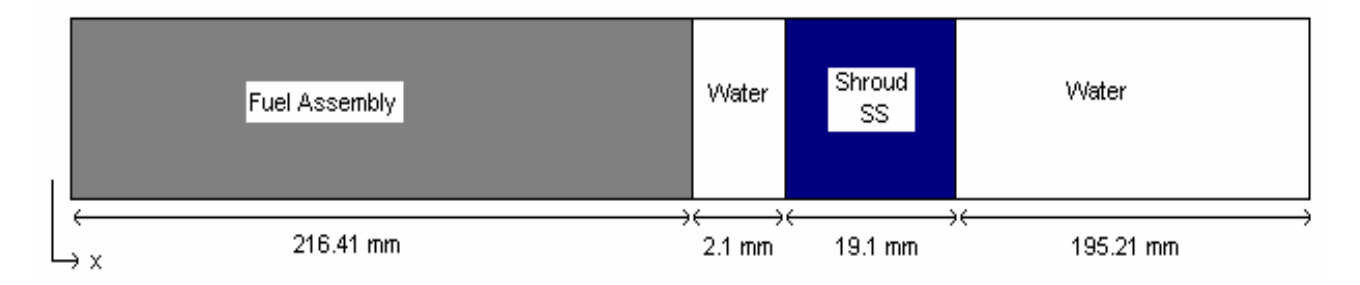


Figure 5 2-D assembly/ reflector model of TMI-PWR [11]

The power distribution in a large (PWR) is significantly affected by the presence of the radial reflector. In the method we use to simulate TMI-PWR reflector, the core, the baffle plate and the water reflector etc. are modeled explicitly, reflecting the complicated geometry of the core/reflector region (see Figure 5 and Table I). The standard model utilized to represent the peripheral zone is to use reflective boundary conditions on the left and the vacuum condition on the right.

Table I TMI-PWR radial reflector material compositions

Material	Composition
Water	H-11.19%; O-88.81%
Shroud	08X18H10T steel

As a final note, the reflector is represented explicitly, however, because the first water layer region is so small compared with the other regions (it is of the order of 2 millimeters thick) we decided to neglect it [4].

3.4 DRAGON simulation models

3.4.1 Pin cell model

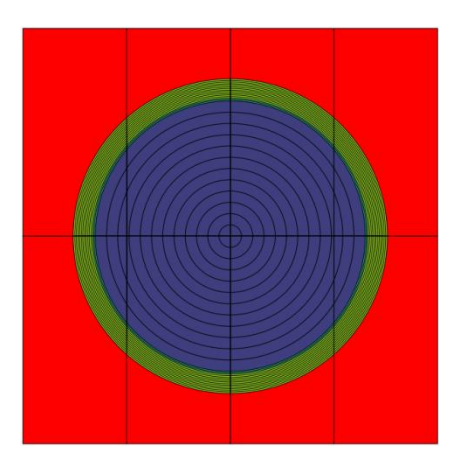


Figure 6 DRAGON TMI-PWR pin cell models

The model is designed to calculate and determine the $k_{\rm eff}$ and the few group cell averaged cross sections. Consequently, we have tried several discretizations for the flux calculation. In fact, Figure 6 shows the DRAGON TMI pin cell model we considered for our simulations. This model includes 8 subdivisions along the Cartesian mesh and 12 radial subdivisions of the fuel region to ensure $k_{\rm eff}$ and flux are spatially converged. The resulting problem to solve involves 96 regions.

3.4.2 Assembly and reflected assembly models

Several models were considered for the TMI-PWR assembly with and without reflector in DRAGON. For boundary conditions, the internal symmetry of the assembly allows us to consider only 1/8 of the assembly. However, for the case of the reflected assembly, the symmetry is reduced to 1/2 of the assembly since there is a vacuum boundary condition on the right of the water reflector region. Note that only reflective boundary conditions are allowed when leakage models (here B1 homogeneous) are considered in DRAGON. Accordingly, we have simulated zero incoming flux boundary conditions on the right of the water reflector by adding a layer containing a mixture of cadmium and vanadium having the same width as that of water reflector. It acts as a strong neutron absorber.

Finally, after several mesh discretization studies for the fuel and reflector regions, we note that the subdivision of the reflective area does not affect considerably the few groups cross sections. In addition, for the worst case it changes the $k_{\rm eff}$ by 80 pcm.

4. Results

The aim of this section is to compare DRAGON results with other already published data [9, 10, and 11]. For this purpose, a pin-cell calculation and 2-D assembly/reflector model of TMI-PWR are considered.

4.1 DRAGON analysis of TMI-PWR pin cell benchmark problem

First, a TYPE K calculation with DRAGON was carried out to obtain the values of the multiplication factor $k_{\rm eff}$ using various WLUP microscopic cross section libraries: JEFF-3.1 ENDF/B-VI.8 and ENDF/B-VII.1 [12]. The results we obtained using DRAGON are then compared with those of MCNP5 [9] in Table II [13].

<u> </u>					
Multiplication factor $(k_{\rm eff})$					
TMI-PWR	ENDF/B-VI.8	ENDF/B-VII.1	JEFF-3.1		
MCNP5	1.43224 +/- 0.00027	1.43536 +/- 0.00022	1.43659 +/- 0.00021		
DRAGON	1.429426	1.43366	1.430623		

Table II k_{eff} for TMI-PWR pin-cell for different cross-section libraries

If we compare the DRAGON results from JEFF-3.1 we observe a significant difference of 600 pcm in the $k_{\rm eff}$ values. For ENDF/B-VI.8, the difference is reduced by a factor of 2 (300 pcm) while for the ENDF/B-VII.1 library, the difference between DRAGON and MCNP5 is below 200 pcm. Consequently, ENDF/B-VII.1 was selected and will be used in the remaining of the paper. Further calculations were performed using DRAGON to generate two-group cell averaged cross sections with the geometry of Figure 6. Two group results are provided in Table III and Table IV respectively.

PWR-HZP Cross Section	MCNP5	WIMSD5[10]	DRAGON
Σ_a^1 (cm-1)	$0.011043 \pm 0.19\%$	0.01104	0.01103
$v\Sigma_f^1 \text{ (cm-1)}$	$0.009881 \pm 2.00\%$	0.009790	0.00971
Σ_a^2 (cm-1)	$0.12044 \pm 0.12\%$	0.1188	0.1174
υ Σ_f^2 (cm-1)	$0.21849 \pm 0.08\%$	0.2168	0.21343
$\Sigma_s^{1-2} \text{ (cm-1)}$	$0.01576 \pm 0.24\%$	0.01568	0.01637

Table III Cell averaged 2 group cross sections

PWR	D(cm)	WIMSD5 Petrovic [8]	T.E.D.M [11]	DRAGON
HZP	D1	1.19677	1.18528	1.18672
	D2	0.37815	0.36604	0.36596

Table IV Cell averaged 2 group diffusion coefficients

We clearly see that there is a good agreement between DRAGON, TDEM and WIMSD5. The maximum error on different cross section and diffusion coefficient is lower than 0.5%.

4.1 2-D TMI-PWR assembly/reflector model

We now consider the 2-D TMI-PWR reflected assembly. The flux calculation is performed with the model shown in Section 3. Here different calculations are performed with vacuum boundary condition on the right of the water region. For the diffusion coefficient calculation we consider a totally reflected assembly with a strong absorber on the right as mentioned in Section 3.4.2.

Figure 7 through 9 compare the thermal and fast scalar flux distribution for fuel, stainless steel and water region generated using DRAGON with those obtained from a MCNP5 simulation [11].

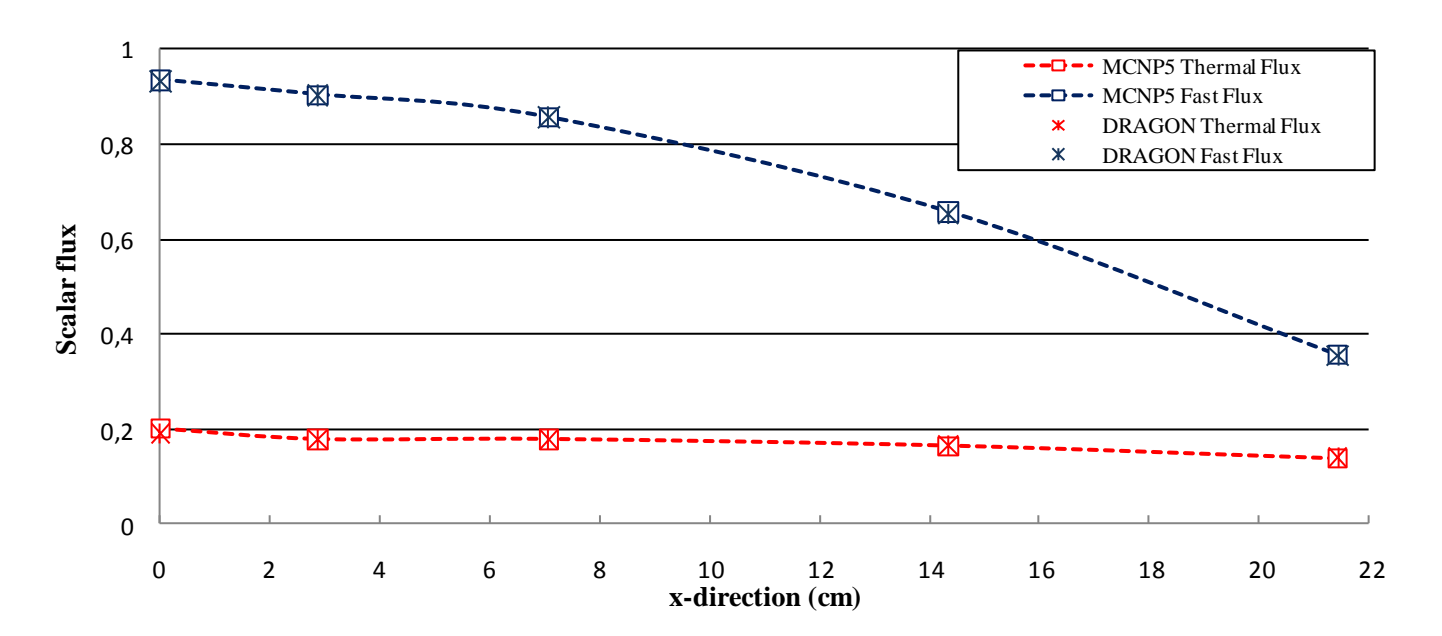


Figure 7 Fuel region scalar flux distribution

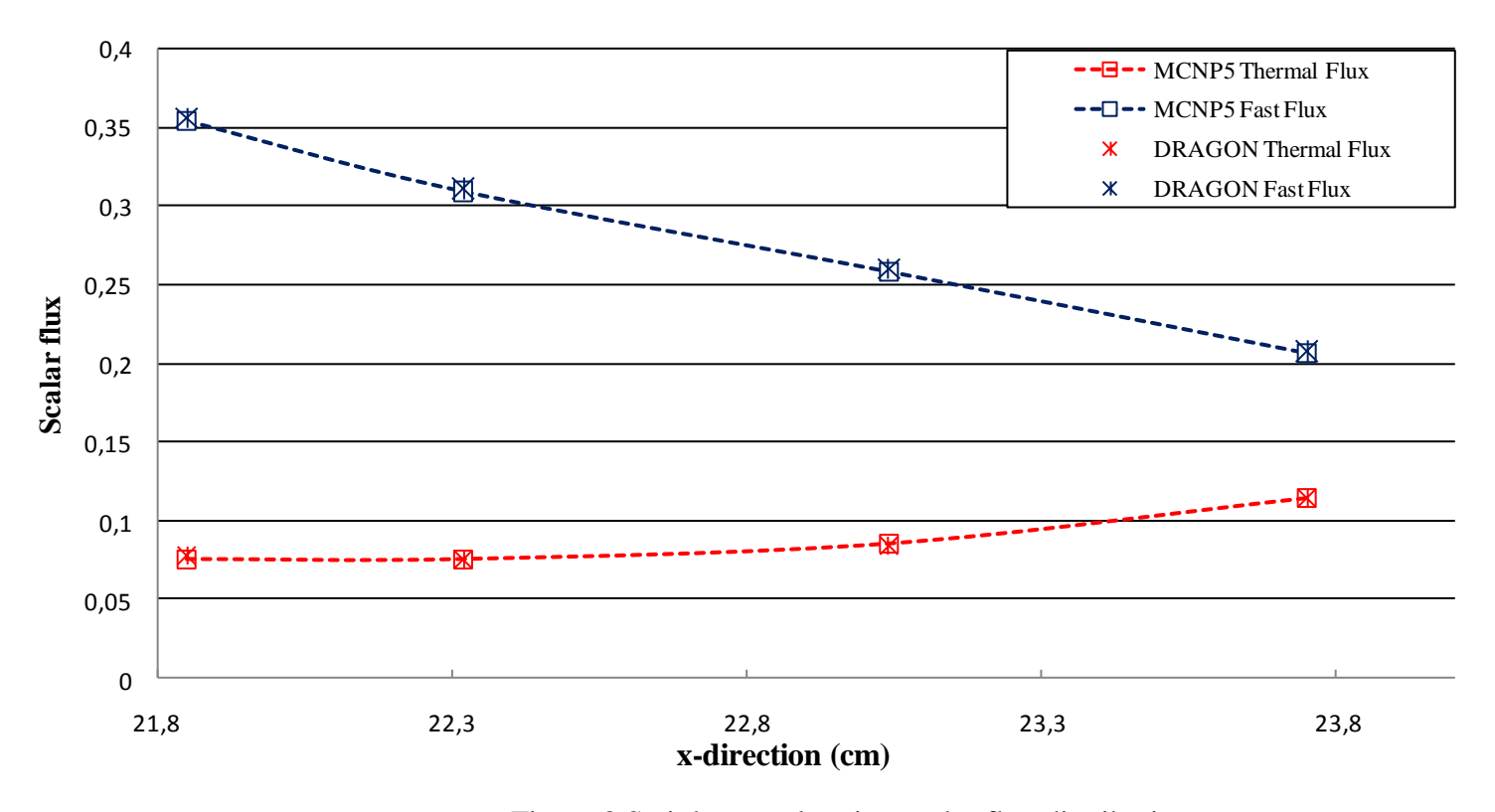


Figure 8 Stainless steel region scalar flux distribution

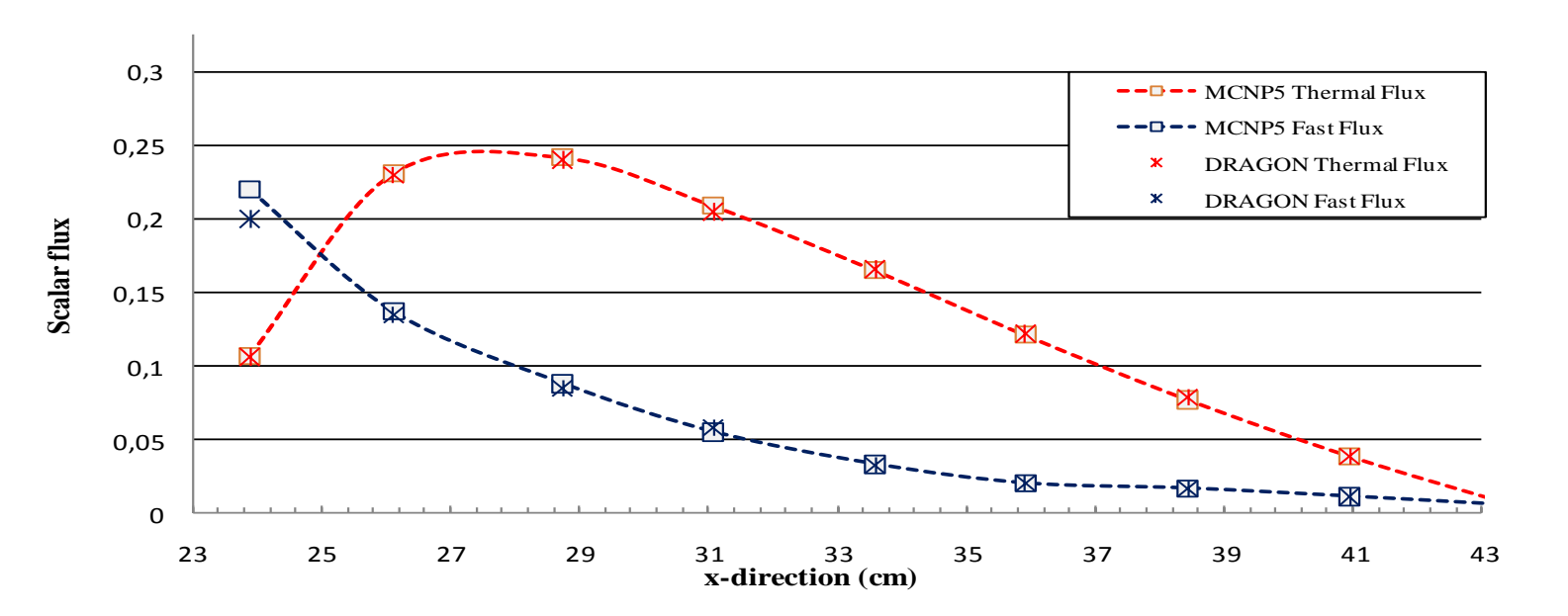


Figure 9 Water region scalar flux distribution

As we can see, there is a maximum relative difference with respect to MCNP5 of 10% for the fast scalar flux in water regions that are in contact with the steel shroud. We also observe a small difference in flux (0.1%) in the water region where the flux reaches its maximum. In fact, this peak is due to the slowing-down of fast neutrons that escape from the fuel and steel region into the thermal energy range. In general, we clearly see that the agreement between DRAGON and MCNP5 is fairly good.

Another interesting point to be studied is the cross sections. Unfortunately, because the MCNP5 cross sections are not available, we have decided to compare our results with those obtained by the transport equivalent diffusion model. Here, we have to note that TDEM uses an equivalence method when condensing the macroscopic cross sections to minimize the difference between analytical solution of diffusion equation and transport solution obtained with MCNP simulation: That is to say, diffusion coefficients and cross sections are arranged. That's why, as we see in Table V, there are differences between DRAGON and TDEM calculations relative to both fuel and reflector regions.

The main differences are observed, on the one hand, for steel down-scattering cross section where the DRAGON result is reduced by a factor of ten relative to that of TDEM. On the other hand, the fuel thermal absorption cross section is increased by 50% compared to that calculated using TDEM. Finally, the TDEM fast absorption cross section for water is about one quarter of that generated with DRAGON.

These differences may explain the interest of using an equivalence model to generate reflector properties when diffusion calculations are considered. However, they do not reflect the reality for transport calculations such as those performed by DRAGON.

Diffusion	Fuel region		Steel region		Water region	
parameter	T.D.E.M	DRAGON	T.D.E.M	DRAGON	T.D.E.M	DRAGON
Σ_a^1 (cm-1)	0.009593	0.01367	0.004719	0.004677	1.03E-04	3.94E-04
Σ_a^2 (cm-1)	0.08799	0.13533	0.1493	0.1508	0.01132	0.01063
$v\Sigma_f^1$ (cm-1)	0.007141	0.008495	0.0	0.0	0.0	0.0
$v\Sigma_f^2$ (cm-1)	0.1487	0.2009	0.0	0.0	0.0	0.0
Σ_s^{1-2} (cm-1)	0.01801	0.01358	0.01403	0.0013	0.053427	0.04875
Σ_s^{2-1} (cm-1)	1.0E-06	1.0E-06	0.0	0.0	0.00024	0.00038
D1	1.4376	1.4379	1.4556	1.4561	1.4705	1.4716
D1	0.8273	0.8279	0.6364	0.637	0.2523	0.2531

Table V Generated material cross sections

4. Conclusions

A survey devoted to the simulation of a radial PWR reflector was submitted in the context of NEA/NSC/DOC (2007)23 benchmark problem. The DRAGON simulation generates two groups diffusion parameters for a reflected assembly. The DRAGON flux distributions were first compared to those obtained using MCNP simulations and show very good agreement. Then the cross sections were compared to those generated for TEDM. Large differences in the cross sections are then observed. We think that these differences are mainly the result of using an equivalence procedure that corrects the cross section for diffusion calculations.

In future work, we intend to use these DRAGON generated two groups diffusion parameters for the fuel assemblies in close contact with the reflector as well as for the reflector itself in DONJON (diffusion code) simulations [14]. For the remaining assemblies we will use conventional burnup dependent assembly properties assuming that those are not affected by the radial reflector. We will thus be able to determine the effect of the reflector on the radial power distribution inside a PWR and compared them with published data.

5. Acknowledgments

One of the authors (N.B.) wishes to express her recognition to Mission Universitaire de Tunisie à Montréal for its financial support. This work was also supported, in part, by a scholarship from the ROASTERS foundation and the Natural Science and Engineering Research Council (NSERC).

6. References

- [1] M. Leroy, P. Leroy, C. Maganaud et al, *Contribution à la qualification de schémas de calcul de REP*. Note interne CEA SERMA/85/1675 (1985).
- [2] J. Mondot, *BETA-Une méthode d'équivalence pour le calcul neutronique des réflecteurs en théorie de la diffusion multigroupe*. Note interne CEA S.E.N/LPN 83/1646 (1983).
- [3] Benchmark for uncertainty analysis in modeling (UAM) for design, operation and safety analysis of LWRs. NEA/NSC/DOC (2007)23.
- [4] M. Blaise, Étude de l'interface cœur-réflecteur, Application au calcul du reflécteur lourd, PhD. Thesis, Paris XI Orsay University (1993).
- [5] G. Marleau, A. Hébert and R. Roy, *A User Guide for DRAGON 3.05*, Report IGE-174 Rev.6, Institut de génie nucléaire, École Polytechnique de Montréal (2006).
- [6] R. Roy, G. Marleau and A. Hébert, "A Cyclic Tracking Procedure for Collision Probability Calculation in 2-D Lattices", *International Topical Meeting Advances in Mathematics, Computations and Reactor Physics*, Pittsburgh, PA, (1991).

- [7] A. Hébert and G. Marleau, "Generalization of the Stamm'ler Method for the Self-Shielding of Resonant Isotopes in Arbitrary Geometries", *Nucl. Sci. Eng.*, 108, 230 (1991).
- [8] I. PETROVIC and P. BENOIST, "BN Theory: Advances and New Models for Neutron Leakage Calculation", *Advances in Nuclear Science and Technology*, 24, 1 (1996).
- [9] *MCNP A General Monte Carlo N-Particle Transport code, Version 5*, Los Alamos National Laboratory (2004).
- [10] J. R. Askew, F. J. Fayers and P. B. Kemshell, "A General Description of the Lattice Code WIMS," *J. Brit. Nucl. Energy Soc.*, 5, 564 (1966).
- [11] Ş. O. Gürdal, "Two-group Diffusion Parameters for LWRs", *Nuclear Energy for New Europe*, Slovenia, 14-17 (2009).
- [12] WIMS Library Update Program, http://www-nds.iaea.org/wimsd/ (2005).
- [13] F.Puente, S.Ghrayeb, *Application of global sensitivity analysis approach to exercise I-1 of the OECD LWR UAM benchmark*. International Conference on Mathematics Computational Methods & Reactor Physics (M&C). New York, (2009).
- [14] E. Varin, A. Hébert, R. ROY and J. KOCLAS, *A User Guide for DONJON 3.01*, Report IGE-208 Rev.4, Institut de génie nucléaire, École Polytechnique de Montréal. (2005).